

# MONTE CARLO WAVEFIELD IMAGING OF 3D PRESTACK DATA

AUTHORS

L. CAZZOLA<sup>1</sup>, E. BONOMI<sup>2</sup>, L. M. BRIEGER<sup>2</sup> and F. ZANOLETTI<sup>1</sup>

Address

ENI, Agip E&P Division, via dell'Unione Europea 1/3, 20097 San Donato Milanese (MI), Italy  
Center For Advanced Studies, Research And Development In Sardinia, CRS4

Submitted to the 63rd EAGE Conference & Exhibition, Amsterdam

## Abstract

We present a new imaging methodology based on the depth extrapolation of a single dataset obtained by randomly compressing sources and shot-gathers. In this work a Monte Carlo imaging condition was implemented with a Phase Shift Plus Interpolation (PSPI) extrapolating kernel and tested on the SEG-EAGE salt model. This study demonstrates that wavefield 3D prestack depth migration is possible for industrial applications, providing high quality results in reasonable computational times.

## Introduction

Prestack depth migration algorithms are usually divided into two classes: wavefield extrapolation techniques based on the implementation of a one-way wave equation solver and Kirchhoff techniques using ray tracing as the wave propagation model. The Kirchhoff approach, based on the eikonal approximation of the scalar wave equation associated with source and receiver location, is recognized as the most flexible method of imaging prestack 3D seismic data; however it may encounter severe imaging inaccuracies in geological situations with fast lateral velocity variations. Wavefield extrapolation techniques are well adapted to common-shot seismic data because in this domain they naturally defined by the correlation two independent propagation problems, one related to the source wavefield and the other to the recorded wavefield, followed by the standard imaging condition. Unfortunately the cost of 3D prestack wavefield extrapolation with tens of thousands of shots is prohibitive.

To obtain a drastic reduction of the computational effort, a new imaging technique based on the simultaneous wavefield extrapolation of many phase-encoded shot-gathers was suggested by S. Morton and C. Ober [1]. In a previous work [2], we analyzed the encoding of sources and common-shot traces with sequences of random numbers. The result of averaging over  $M$  such depth migrations provides a map of the correct reflectivity hidden among a large number of spurious terms that vanish in the limit of large  $M$ . This technique is valid for any  $M$  sequences of random numbers independently drawn from a given probability distribution with mean value zero and variance one. With this method, for a prestack migration involving tens of thousands of shots, the number of migrations necessary to capture a good reflectivity map is only a small fraction of the number of shots.

## Theory

Migration is an inversion process which reconstructs the map  $R(\mathbf{x}, z)$  of local reflectivity from the velocity field  $c(\mathbf{x}, z)$  and the prestack seismic volume  $Q(\mathbf{x}_s, \mathbf{x}_g, t) = p(\mathbf{x}_s, \mathbf{x}_g, z=0, t)$ , where  $p(\mathbf{x}_s, \mathbf{x}_g, 0, t)$  denotes the pressure measured at time  $t$  by a receiver position  $(\mathbf{x}_g, z)$  after the emission of an impulsive source at position  $(\mathbf{x}_s, z)$  has been initiated at  $t=0$ . In the case of a sequence of  $N$  independent shots, the seismic volume is written:

$$(1) \quad Q(\mathbf{x}_s, \mathbf{x}_g, t) = \sum_{n=1}^N \mathbf{d}\mathbf{x}_s - s_n T_n(\mathbf{x}_g, t)$$

where  $s_n$  is the source position at the  $n$ -th shot and  $T_n$  represents the resulting field of recorded traces. The basic strategy for prestack wavefield migration is to formulate the wave propagation in the space-frequency domain. Linearity of the one-way equation and its formulation in the *field coordinate* system allows the uncoupling of the downward extrapolation of the seismic volume, Eq.(1), in two depth wavefield propagations, one for the source,  $p_s$ , and the other for the shot-gather,  $p_g$ . The only coupling between them is introduced through the *imaging condition* from which the map of the local reflectivity  $R(\mathbf{x}, z) = p(\mathbf{x}, \mathbf{x}, z, t=0)$  is derived. For a sequence of  $N$  shots migrated independently, the expression for  $R$  at each depth  $j\Delta z$  takes the canonical form:

$$(2) \quad R(\mathbf{x}, j\Delta z) = \sum_{n=1}^N \sum_{\mathbf{w}} \overline{\widehat{p}_s^{(n)}}(\mathbf{x}, j\Delta z, \mathbf{w}) \widehat{p}_g^{(n)}(\mathbf{x}, j\Delta z, \mathbf{w})$$

where  $\widehat{p}_s^{(n)}$  denotes the acoustic wave field produced by the impulsive source wavelet  $p_s^{(n)}(\mathbf{x}_s, 0, t) = \mathbf{d}(\mathbf{x}_s - s_n) \mathbf{d}(t)$  in the space-frequency domain, and, similarly,  $\widehat{p}_g^{(n)}$  denotes the depth extrapolation of the shot gather  $p_g^{(n)}(\mathbf{x}_g, 0, t) = T_n(\mathbf{x}_g, t)$ . In marine surveys  $N$  can be tens of thousands of shots; Eq.(2) eloquently illustrate the computational cost of prestack imaging. To drastically reduce the processing, sources and seismic data are compressed in the space-frequency domain: a unique source term is composed of a linear combination of all source wavelets and a unique gather of seismic traces is assembled by superposing all shot gathers. The resulting compressed seismic volume which serves as the initial condition of the depth extrapolation, is:

$$(3) \quad \widehat{Q}(\mathbf{x}_s, \mathbf{x}_g, \mathbf{w}) = \sum_{n,n'}^N a_{w,n} \mathbf{d}(\mathbf{x}_s - s_n) a_{w,n'} \widehat{T}_{n'}(\mathbf{x}_g, \mathbf{w})$$

where each coefficient  $a_{w,n}$  is a complex weight. The usual imaging condition gives the following map of local reflectivity  $r$ :

$$(4) \quad r(\mathbf{x}, j\Delta z) = \sum_{n=1}^N \sum_{\mathbf{w}} |a_{w,n}|^2 \overline{\widehat{p}_s^{(n)}}(\mathbf{x}, j\Delta z, \mathbf{w}) \widehat{p}_g^{(n)}(\mathbf{x}, j\Delta z, \mathbf{w}) + \sum_{n \neq n'}^N \sum_{\mathbf{w}} \overline{a_{w,n}} a_{w,n'} \overline{\widehat{p}_s^{(n)}}(\mathbf{x}, j\Delta z, \mathbf{w}) \widehat{p}_g^{(n')}(\mathbf{x}, j\Delta z, \mathbf{w})$$

If now the collection  $a_{w,n}$  forms a suite of *independent, identical random variables*, then the stochastic mean value of  $r$  takes the form:

$$(5) \quad \langle r \rangle(\mathbf{x}, j\Delta z) = \langle |a|^2 \rangle \sum_{n=1}^N \sum_{\mathbf{w}} \overline{\widehat{p}_s^{(n)}}(\mathbf{x}, j\Delta z, \mathbf{w}) \widehat{p}_g^{(n)}(\mathbf{x}, j\Delta z, \mathbf{w}) + \langle |a \rangle^2 \sum_{n \neq n'}^N \sum_{\mathbf{w}} \overline{\widehat{p}_s^{(n)}}(\mathbf{x}, j\Delta z, \mathbf{w}) \widehat{p}_g^{(n')}(\mathbf{x}, j\Delta z, \mathbf{w})$$

with  $\langle |a|^2 \rangle$  denoting the mean value of the squared modulus of the random variable  $a$ , and  $\langle |a \rangle^2$  denoting the squared modulus of the mean value. For *any* probability distribution such that  $\langle a \rangle = 0$  and  $\langle |a|^2 \rangle = 1$ , the expectation value of  $r$  in Eq.(5) gives exactly the imaging condition for  $N$  independent shots,  $\langle r \rangle(\mathbf{x}, j\Delta z) = R(\mathbf{x}, j\Delta z)$ , and then the correct reflectivity of the medium is thus recovered.

## Methodology

To obtain a numerical estimate of reflectivity, a Monte Carlo importance sampling approach [3] can be used. More precisely, we run a sequence of  $M$  depth migrations, starting each time from a new randomly compressed seismic volume and we construct the sequence  $r_1, r_2, \dots, r_M$  of images to form the arithmetic mean

$$(6) \quad A_M(\mathbf{x}, j\Delta z) = \frac{1}{M} \sum_{m=1}^M r_m(\mathbf{x}, j\Delta z).$$

Monte Carlo theory states that, as  $M$  increases the variance of the mean value of  $A_M$  decreases pointwise as  $M^{-1}$ . In other words, when the number of migrations increases, the following pointwise limit  $\lim_{M \rightarrow \infty} A_M = \langle r \rangle$  almost surely exists. In ref. [2], this result was tested with random coefficients  $a_{w,n}$  sampled in three different distributions:

- a)  $a = \exp i\mathbf{q}$  with  $\mathbf{q}$  uniformly distributed in  $[0, 2\pi)$ ;
- b) gaussian distribution with mean 0 and variance 1;
- c)  $a = \pm 1$  with probability  $1/2$

Computer experiments show that these three compression methods are all reliable in the sense that they provide an image comparable to that obtained with the standard shot-by shot prestack migration. The accuracy is only controlled by the number  $M$  of stacked migrations which can remain much smaller than  $N$ , the number of shot gathers. Since the cost of migrating a single shot or a random superposition of many shots is the same, the Monte Carlo approach allows the accuracy of wavefield migration at an acceptable computing cost. This savings of time enables to take advantage of the accurate, but costly, PSPI downward extrapolator. PSPI is a practical alternative to others forms of migration, as long as the set of reference velocities is well chosen. A selection mechanism, described in [4], was devised to highlight a minimal set of velocity values that predominate statistically in the propagation process. The resulting economy translates into an important reduction in computational time for each depth extrapolation.

### SEG-EAGE salt model

The SEG-EAGE Narrow Angle dataset (C3-NA) was chosen to illustrate the capabilities of the Monte Carlo imaging method coupled to the PSPI downward extrapolation in comparison to a standard Kirchhoff package. Figure 1 displays the crossline 250 where the artifacts in the salt base, present only in the Kirchhoff migration, disappear with the PSPI and the Monte Carlo imaging which, in addition, adequately reconstruct the steep dipping flanks of the salt body. In figure 2, crossline 350, it is shown that caustics, which plague Kirchhoff migration, do not affect at all the result obtained with the presented method. Images of fig. 1 (left) and 2 (left) have been extracted when Monte Carlo code reached about the same CPU time requested by Kirchhoff migration for imaging the same volume (140 iterations). The drawback of the Monte Carlo approach is the background noise intrinsic to this algorithm which can be, nevertheless, controlled by increasing the number of images used to approximate  $\langle r \rangle$ , Eq.(6), as it is displayed in fig. 3 where crossline 350 is shown after 280 iterations.

### Acknowledgments

We wish to thank ENI-Agip E&P division for permission to publish, Patrizia Cibin for providing the Kirchhoff migration results and, Luca Bertelli and Cesare Alberti di Catenaja for their encouragement.

### References

- [1] S. A. Morton and C. C. Ober, 1998, *Faster shot-record depth migrations using phase encoding*, 68<sup>th</sup> Ann. Internat. Mtg., Soc. Expl. Geophys., Expanded Abstracts.
- [2] E. Bonomi and L. Cazzola, 1999, *Prestack imaging of compressed seismic data: a Monte Carlo approach*, 69<sup>th</sup> Ann. Internat. Mtg., Soc. Expl. Geophys., Expanded Abstracts.
- [3] M. H. Kalos and P. A. Whitlock, 1986, *Monte Carlo methods*, Volume 1: basics, John Wiley and Sons.
- [4] E. Bonomi, L. M. Brieger, C. Nardone, E. Pieroni, 1998, *Phase Shift Plus Interpolation: a scheme for high-performance echo-reconstructive imaging*, Computers in physics, **12**, No. 2.

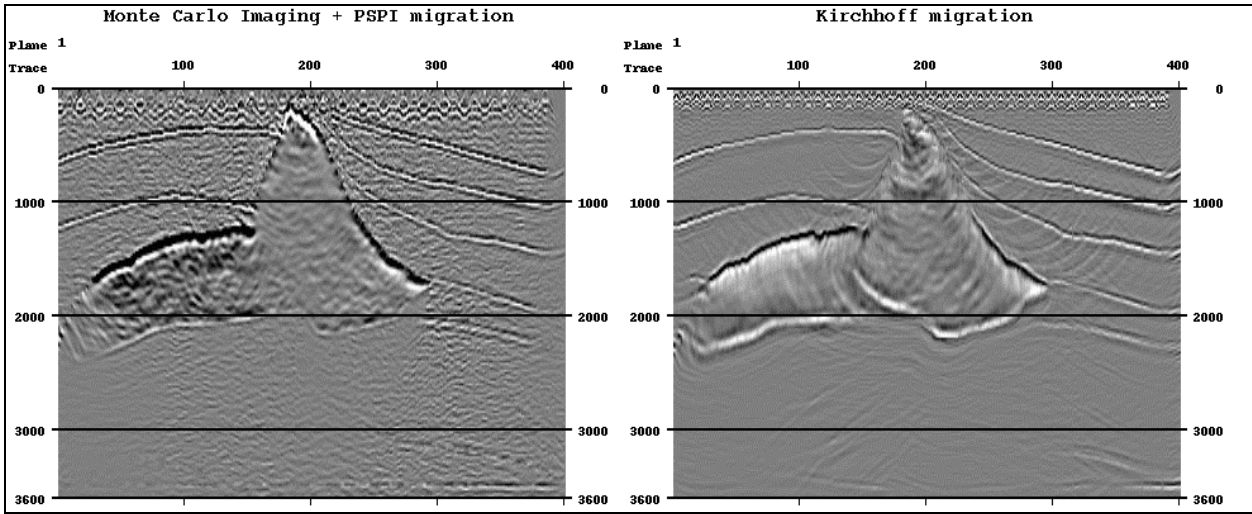


Fig. 1. Crossline 250 of SEG-EAGE salt model. The artifacts in the salt base, present in the Kirchhoff migration (right), disappear with the PSPI and the Monte Carlo imaging (left) which, in addition, adequately reconstruct the steep dipping flanks of the salt body. This image has been extracted after  $M=140$  iterations.

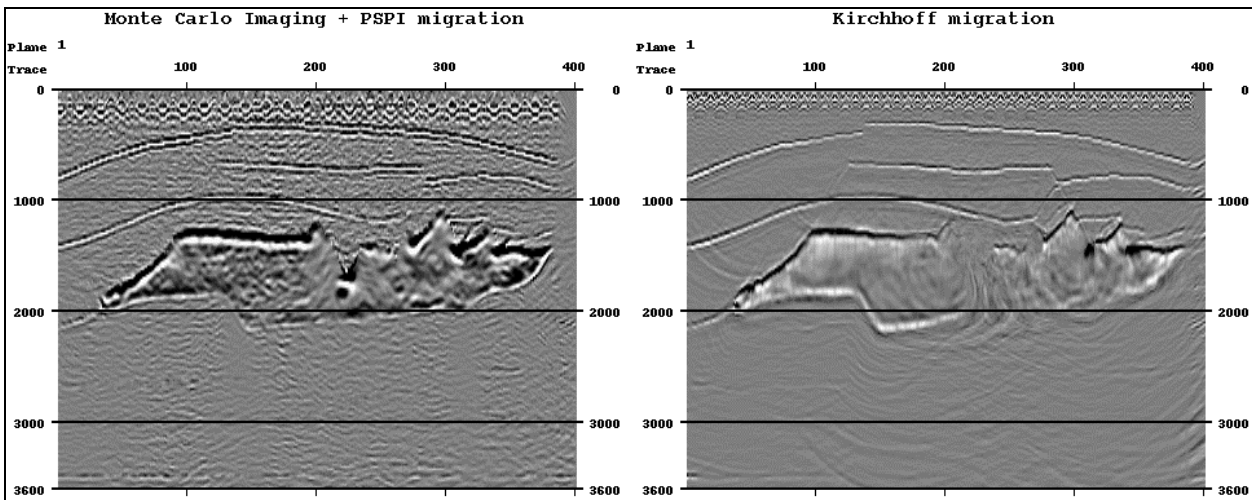


Fig. 2. Crossline 350 of SEG-EAGE salt model. Kirchhoff migration (right) is unable to correctly define the salt base because of the multiple ray-paths generated by the corrugated salt top. PSPI migration and the Monte Carlo imaging (left) is not affected at all by this problem. This image has been extracted after  $M=140$  iterations.

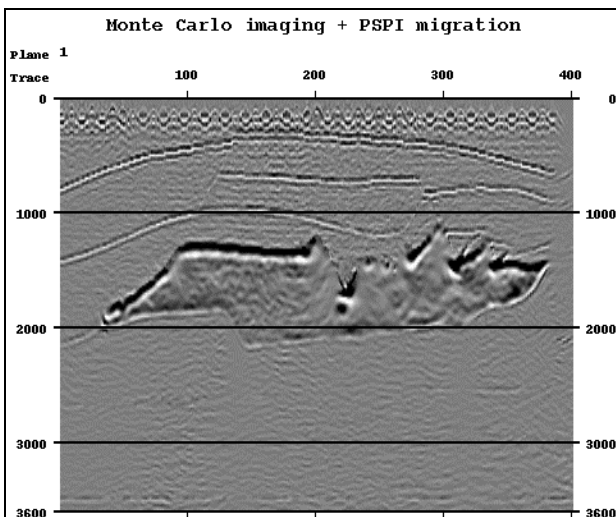


Fig. 3. Image of crossline 350 of SEG-EAGE salt model obtained after  $M=280$  iterations. Overall image is more focused and faint events, as the faults over the salt and the sand lens, appear from the background noise.